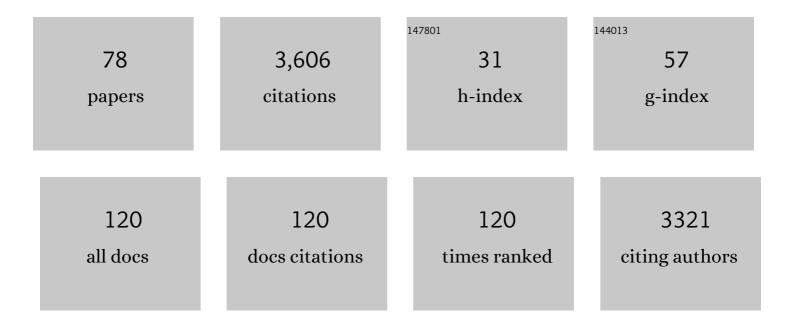
## Francien Peterse

List of Publications by Year in descending order

Source: https://exaly.com/author-pdf/1811789/publications.pdf Version: 2024-02-01



#	Article	IF	CITATIONS
1	Limited Lateral Transport Bias During Export of Sea Surface Temperature Proxy Carriers in the Mediterranean Sea. Geophysical Research Letters, 2022, 49, .	4.0	5
2	Soil pH and aridity influence distributions of branched tetraether lipids in grassland soils along an aridity transect. Organic Geochemistry, 2022, 164, 104347.	1.8	12
3	Distinct sources of bacterial branched GMGTs in the Godavari River basin (India) and Bay of Bengal sediments. Organic Geochemistry, 2022, , 104405.	1.8	4
4	Multiproxy records of temperature, precipitation and vegetation on the central Chinese Loess Plateau over the past 200,000 years. Quaternary Science Reviews, 2022, 288, 107579.	3.0	6
5	Synchronous vegetation response to the last glacial-interglacial transition in northwest Europe. Communications Earth & Environment, 2022, 3, .	6.8	6
6	Rapid expansion of meso-megathermal rain forests into the southern high latitudes at the onset of the Paleocene-Eocene Thermal Maximum. Geology, 2021, 49, 40-44.	4.4	24
7	Multiscale Microbial Preservation and Biogeochemical Signals in a Modern Hot-Spring Siliceous Sinter Rich in CO2 Emissions, KrýsuvÃk Geothermal Field, Iceland. Minerals (Basel, Switzerland), 2021, 11, 263.	2.0	3
8	Identifying marine and freshwater overprints on soil-derived branched GDGT temperature signals in Pliocene Mississippi and Amazon River fan sediments. Organic Geochemistry, 2021, 154, 104200.	1.8	7
9	Anoxic in situ production of bacterial GMGTs in the water column and surficial bottom sediments of a meromictic tropical crater lake: Implications for lake paleothermometry. Geochimica Et Cosmochimica Acta, 2021, 306, 171-188.	3.9	3
10	Massive and rapid predominantly volcanic CO <sub>2</sub> emission during the end-Permian mass extinction. Proceedings of the National Academy of Sciences of the United States of America, 2021, 118,	7.1	35
11	Temperature, precipitation, and vegetation changes in the Eastern Mediterranean over the last deglaciation and Dansgaard-Oeschger events. Palaeogeography, Palaeoclimatology, Palaeoecology, 2021, 577, 110535.	2.3	3
12	The influence of soil chemistry on branched tetraether lipids in mid- and high latitude soils: Implications for brGDGT- based paleothermometry. Geochimica Et Cosmochimica Acta, 2021, 310, 95-112.	3.9	34
13	Sedimentary Branched Tetraethers in an African Lake Record 170 KYR of Tropical Temperature Change: Assessment of Calibrations. , 2021, , .		0
14	Seasonal and multi-annual variation in the abundance of isoprenoid GDGT membrane lipids and their producers in the water column of a meromictic equatorial crater lake (Lake Chala, East Africa). Quaternary Science Reviews, 2021, 273, 107263.	3.0	18
15	Maastrichtian–Rupelian paleoclimates in the southwest Pacific – a critical re-evaluation of biomarker paleothermometry and dinoflagellate cyst paleoecology at Ocean Drilling Program Site 1172. Climate of the Past, 2021, 17, 2393-2425.	3.4	14
16	BayMBT: A Bayesian calibration model for branched glycerol dialkyl glycerol tetraethers in soils and peats. Geochimica Et Cosmochimica Acta, 2020, 268, 142-159.	3.9	110
17	From Andes to Amazon: Assessing Branched Tetraether Lipids as Tracers for Soil Organic Carbon in the Madre de Dios River System. Journal of Geophysical Research G: Biogeosciences, 2020, 125, e2019JC005270.	3.0	17
18	Validation and calibration of soil δ2H and brGDGTs along (E-W) and strike (N-S) of the Himalayan climatic gradient. Geochimica Et Cosmochimica Acta, 2020, 290, 408-423.	3.9	6

#	Article	IF	CITATIONS
19	Links between microbial biomass and necromass components in the top- and subsoils of temperate grasslands along an aridity gradient. Geoderma, 2020, 379, 114623.	5.1	18
20	A Warm, Stratified, and Restricted Labrador Sea Across the Middle Eocene and Its Climatic Optimum. Paleoceanography and Paleoclimatology, 2020, 35, e2020PA003932.	2.9	12
21	Recovery from multiâ€millennial natural coastal hypoxia in the Stockholm Archipelago, Baltic Sea, terminated by modern human activity. Limnology and Oceanography, 2020, 65, 3085-3097.	3.1	6
22	A new age model for the Pliocene of the southern North Sea basin: a multi-proxy climate reconstruction. Climate of the Past, 2020, 16, 523-541.	3.4	4
23	Seasonal and spatial variability in δ18O and δD values in waters of the Godavari River basin: Insights into hydrological processes. Journal of Hydrology: Regional Studies, 2020, 30, 100706.	2.4	7
24	Preferential degradation of leaf- vs. root-derived organic carbon in earthworm-affected soil. Geoderma, 2020, 372, 114391.	5.1	12
25	Assessing branched tetraether lipids as tracers of soil organic carbon transport through the Carminowe Creek catchment (southwest England). Biogeosciences, 2020, 17, 3183-3201.	3.3	18
26	Seasonal variability and sources of in situ brGDGT production in a permanently stratified African crater lake. Biogeosciences, 2020, 17, 5443-5463.	3.3	31
27	Lessons from a high-CO <sub>2</sub> world: an ocean view from  â^¼â€‰3Âr years ago. Climate of the Past, 2020, 16, 1599-1615.	njllion 3.4	52
28	Surface-circulation change in the southwest Pacific Ocean across the Middle Eocene Climatic Optimum: inferences from dinoflagellate cysts and biomarker paleothermometry. Climate of the Past, 2020, 16, 1667-1689.	3.4	17
29	Late Paleocene–early Eocene Arctic Ocean sea surface temperatures: reassessing biomarker paleothermometry at Lomonosov Ridge. Climate of the Past, 2020, 16, 2381-2400.	3.4	22
30	Production of branched tetraethers in the marine realm: Svalbard fjord sediments revisited. Organic Geochemistry, 2019, 138, 103907.	1.8	15
31	Lipid biomarker temperature proxy responds to abrupt shift in the bacterial community composition in geothermally heated soils. Organic Geochemistry, 2019, 137, 103897.	1.8	78
32	Late Quaternary climate variability at Mfabeni peatland, eastern South Africa. Climate of the Past, 2019, 15, 1153-1170.	3.4	20
33	Compositional Characteristics of Fluvial Particulate Organic Matter Exported From the World's Largest Alpine Wetland. Journal of Geophysical Research G: Biogeosciences, 2019, 124, 2709-2727.	3.0	3
34	Harmful algae and export production collapse in the equatorial Atlantic during the zenith of Middle Eocene Climatic Optimum warmth. Geology, 2019, 47, 247-250.	4.4	21
35	Arctic vegetation, temperature, and hydrology during Early Eocene transient global warming events. Global and Planetary Change, 2019, 178, 139-152.	3.5	68
36	Widespread Warming Before and Elevated Barium Burial During the Paleoceneâ€Eocene Thermal Maximum: Evidence for Methane Hydrate Release?. Paleoceanography and Paleoclimatology, 2019, 34, 546-566.	2.9	33

#	Article	IF	CITATIONS
37	Earthworms act as biochemical reactors to convert labile plant compounds into stabilized soil microbial necromass. Communications Biology, 2019, 2, 441.	4.4	77
38	Late Holocene changes in vegetation and atmospheric circulation at Lake Uddelermeer (The) Tj ETQq0 0 0 rgB <sup>-</sup> Quaternary Science, 2018, 33, 100-111.	Г /Overlock 2.1	10 Tf 50 707 10
39	Using tetraether lipids archived in North Sea Basin sediments to extract North Western European Pliocene continental air temperatures. Earth and Planetary Science Letters, 2018, 490, 193-205.	4.4	46
40	Evolution of biomolecular loadings along a major river system. Geochimica Et Cosmochimica Acta, 2018, 223, 389-404.	3.9	34
41	Reconciling drainage and receiving basin signatures of the Godavari River system. Biogeosciences, 2018, 15, 3357-3375.	3.3	19
42	Organic matter characteristics in yedoma and thermokarst deposits on Baldwin Peninsula, west Alaska. Biogeosciences, 2018, 15, 6033-6048.	3.3	28
43	Paleoceanography and ice sheet variability offshore Wilkes Land, Antarctica – Part 3: Insights from Oligocene–Miocene TEX <sub>86</sub> -based sea surface temperature reconstructions. Climate of the Past, 2018, 14, 1275-1297.	3.4	42
44	Long-chain diols in rivers: distribution and potential biological sources. Biogeosciences, 2018, 15, 4147-4161.	3.3	15
45	Land–sea coupling of early Pleistocene glacial cycles in the southern North Sea exhibit dominant Northern Hemisphere forcing. Climate of the Past, 2018, 14, 397-411.	3.4	15
46	Synchronous tropical and polar temperature evolution in the Eocene. Nature, 2018, 559, 382-386.	27.8	185
47	Robust multi-proxy data integration, using late Cretaceous paleotemperature records as a case study. Earth and Planetary Science Letters, 2018, 500, 215-224.	4.4	24
48	Seasonal variability in the abundance and stable carbon-isotopic composition of lipid biomarkers in suspended particulate matter from a stratified equatorial lake (Lake Chala, Kenya/Tanzania): Implications for the sedimentary record. Quaternary Science Reviews, 2018, 192, 208-224.	3.0	57
49	Constraining Instantaneous Fluxes and Integrated Compositions of Fluvially Discharged Organic Matter. Geochemistry, Geophysics, Geosystems, 2018, 19, 2453-2462.	2.5	13
50	Biomarkers in <scp>L</scp> ake <scp>V</scp> an sediments reveal dry conditions in eastern <scp>A</scp> natolia during 110.000–10.000 years <scp>B</scp> . <scp>P</scp> Geochemistry, Geophysics, Geosystems, 2017, 18, 571-583.	2.5	20
51	Latest Cretaceous climatic and environmental change in the South Atlantic region. Paleoceanography, 2017, 32, 466-483.	3.0	51
52	Astronomical age constraints and extinction mechanisms of the Late Triassic Carnian crisis. Scientific Reports, 2017, 7, 2557.	3.3	61
53	Branched GDGT signals in fluvial sediments of the Danube River basin: Method comparison and longitudinal evolution. Organic Geochemistry, 2017, 103, 88-96.	1.8	30
54	Grain Size Associations of Branched Tetraether Lipids in Soils and Riverbank Sediments: Influence of Hydrodynamic Sorting Processes. Frontiers in Earth Science, 2017, 5, .	1.8	14

#	Article	IF	CITATIONS
55	Organic carbon isotope and molecular fossil records of vegetation evolution in central Loess Plateau since 450 kyr. Science China Earth Sciences, 2016, 59, 1206-1215.	5.2	15
56	Late Pleistocene climate evolution in Southeastern Europe recorded by soil bacterial membrane lipids in Serbian loess. Palaeogeography, Palaeoclimatology, Palaeoecology, 2016, 449, 141-148.	2.3	21
57	A laboratory experiment on the behaviour of soil-derived core and intact polar GDGTs in aquatic environments. Biogeosciences, 2015, 12, 933-943.	3.3	16
58	Sources of organic matter in Changjiang (Yangtze River) bed sediments: Preliminary insights from organic geochemical proxies. Organic Geochemistry, 2015, 85, 11-21.	1.8	36
59	Late Pliocene–Pleistocene expansion of C4 vegetation in semiarid East Asia linked to increased burning. Geology, 2014, 42, 1067-1070.	4.4	32
60	Sources of glycerol dialkyl glycerol tetraethers (GDGTs) in catchment soils, water column and sediments of Lake Rotsee (Switzerland) – Implications for the application of GDGT-based proxies for lakes. Organic Geochemistry, 2014, 66, 164-173.	1.8	64
61	Molecular records of continental air temperature and monsoon precipitation variability in East Asia spanning the past 130,000 years. Quaternary Science Reviews, 2014, 83, 76-82.	3.0	118
62	Tracing the methane cycle with lipid biomarkers in Lake Rotsee (Switzerland). Organic Geochemistry, 2014, 66, 174-181.	1.8	49
63	Branched glycerol dialkyl glycerol tetraethers in Arctic lake sediments: Sources and implications for paleothermometry at high latitudes. Journal of Geophysical Research G: Biogeosciences, 2014, 119, 1738-1754.	3.0	46
64	Biomarkers record environmental changes along an altitudinal transect in the wettest place on Earth. Organic Geochemistry, 2013, 60, 93-99.	1.8	48
65	An interlaboratory study of TEX <sub>86</sub> and BIT analysis of sediments, extracts, and standard mixtures. Geochemistry, Geophysics, Geosystems, 2013, 14, 5263-5285.	2.5	76
66	Revised calibration of the MBT–CBT paleotemperature proxy based on branched tetraether membrane lipids in surface soils. Geochimica Et Cosmochimica Acta, 2012, 96, 215-229.	3.9	369
67	Lowâ€ammonia niche of ammoniaâ€oxidizing archaea in rotating biological contactors of a municipal wastewater treatment plant. Environmental Microbiology, 2012, 14, 2589-2600.	3.8	82
68	Absence of seasonal patterns in MBT–CBT indices in mid-latitude soils. Geochimica Et Cosmochimica Acta, 2011, 75, 3179-3190.	3.9	113
69	Decoupled warming and monsoon precipitation in East Asia over the last deglaciation. Earth and Planetary Science Letters, 2011, 301, 256-264.	4.4	204
70	Identification and distribution of intact polar branched tetraether lipids in peat and soil. Organic Geochemistry, 2011, 42, 1007-1015.	1.8	66
71	Large ancient organic matter contributions to Arctic marine sediments (Svalbard). Limnology and Oceanography, 2011, 56, 1463-1474.	3.1	51
72	Contribution of riverâ€borne soil organic carbon to the Gulf of Lions (NW Mediterranean). Limnology and Oceanography, 2010, 55, 507-518.	3.1	21

#	Article	IF	CITATIONS
73	Influence of soil pH on the abundance and distribution of core and intact polar lipid-derived branched GDGTs in soil. Organic Geochemistry, 2010, 41, 1171-1175.	1.8	105
74	Contribution of river-borne soil organic carbon to the Gulf of Lions (NW Mediterranean). Limnology and Oceanography, 2010, 55, 507-518.	3.1	23
75	Assessment of soil <i>n</i> -alkane Î′ <i>D</i> and branched tetraether membrane lipid distributions as tools for paleoelevation reconstruction. Biogeosciences, 2009, 6, 2799-2807.	3.3	79
76	Distribution of branched tetraether lipids in geothermally heated soils: Implications for the MBT/CBT temperature proxy. Organic Geochemistry, 2009, 40, 201-205.	1.8	54
77	Constraints on the application of the MBT/CBT palaeothermometer at high latitude environments (Svalbard, Norway). Organic Geochemistry, 2009, 40, 692-699.	1.8	232
78	Soil organic matter chemistry in allophanic soils: a pyrolysis-GC/MS study of a Costa Rican Andosol catena. European Journal of Soil Science, 2007, 58, 1330-1347.	3.9	175